Nonlinear magnetic stochastic resonance: Noise-strength–constant-force diagrams

Yu. L. Raikher* and V. I. Stepanov
Institute of Continuous Media Mechanics, Urals Branch of RAS, 614013 Perm, Russia

A. N. Grigorenko and P. I. Nikitin
General Physics Institute, RAS, 117492 Moscow, Russia

(Received 16 June 1997)

Signal-to-noise properties of a periodically driven noisy magnetic bistable system—superparamagnetic particles with uniaxial anisotropy—are investigated in the framework of the Fokker-Planck equation solved both analytically and numerically. The system is subject to a constant (bias) field that imparts even harmonics into its low-frequency magnetic spectrum. A comparative study of the linear and quadratic susceptibilities and stochastic resonances (SR) is carried out. We show that the quadratic SR is much sharper than the linear one and unlike the latter is essentially frequency dependent. [S1063-651X(97)10411-1]

PACS number(s): 05.40.+j, 75.50.Tt, 05.45.+b

INTRODUCTION

The phenomenon called in a modern thesaurus *the stochastic resonance* (SR) has by now shaped up into a general concept appealing to a great many researchers in diverse fields. Having been taken into collective development, it has proved to be rather fruitful. By now the number of papers on stochastic resonance is in the hundreds, and overall review articles [1–3] are beginning to appear.

SR is a kinetic effect universally inherent to bistable or multistable dynamic systems with white or color noise. Its main manifestation is the appearance of a maximum on the noise intensity dependences of the signal-to-noise ratio in a system subject to a weak driving force. Essentially, this behavior is due to the presence of an exponential Kramers time $\tau \propto \exp(\Delta U/D)$ of the system switching between energy minima; here ΔU is the effective height of the energy barrier separating the potential wells and D is the noise intensity.

For the most part, magnetic systems are multistable. Therefore, the idea of the magnetic stochastic resonance has emerged in a natural way first as a theoretical matter [4,5] (see also Ref. [6]), shortly afterward supported by experimental evidence [7,8]. In Refs. [9] and [10], an accurate approach to the magnetic SR in the framework of the linear response theory was developed.

Micromagnetism as defined by Brown [11] is the branch of magnetic science that studies the properties of fine ferromagnetic particles. For such particles in the size range ~ 10 nm the height of the internal magnetic anisotropy barrier ΔU_a is comparable to the thermal excitation strength $k_B T$. Due to that, the magnetic moment $\boldsymbol{\mu}$ of a single-domain particle begins to spontaneously wander between two (uniaxial case) or numerous (cubic case) anisotropy energy U_a minima [12,13]. This motion manifests itself as a magnetic relaxation with the characteristic time $\tau \propto \exp(\Delta U_a/k_B T)$, i.e., the well-known *superparamagnetism* phenomenon that has been under study for quite some time, see Ref. [14] for a state-of-the-art review.

The meaning of the generic SR terms as applied to a single-domain superparamagnetic particle (or an assembly of those) is apparent. The dynamic variable is connected to the orientation of magnetic moment, the background noise is thermal and thus white, and the excitation is created by a weak external harmonic magnetic field $H_p(t) = H_{p0}\exp(i\Omega t)$. The signal is the responding dynamic magnetization $M(t)$ in the direction of $\mathbf{H}_p$ and the signal-to-noise ratio is defined through the spectral power density $Q(\omega)$ of $M(t)$ at some given frequency. We remark that from the experimental viewpoint all the quantities involved can be feasibly measured by conventional techniques.

In Ref. [7] the importance of a constant field (imposed on the system along its anisotropy axis) on the magnetic SR is demonstrated. First quantitative results on this effect in a superparamagnetic particle assembly are given in Ref. [10]. The ''constant force'' $\mathbf{H}$ enters the energy function as the term $-\boldsymbol{\mu}\cdot\mathbf{H}$. For a uniaxial anisotropy, i.e., initially symmetrical bistable system, the bias field removes the degeneracy and makes the potential wells nonequivalent. The gradual increase of H enlarges this deformation and finally transforms a two-well potential into a one-well one.

The bias-field effect has two main aspects of interest. First, it considerably affects the usual SR behavior determined by the linear response $M(t) \propto \exp(i\Omega t)$. Second, the break of symmetry adds even terms into the frequency content of $M(t)$, which otherwise consists only of odd harmonics. Thus one gets an opportunity to examine a nonlinear response in its most simple (quadratic) form $M^{(2)}(t) \propto H_{p0}^2 \exp(2i\Omega t)$. The latter is the subject of our particular interest. Indeed, at least since the time of the boom in studies of spin glasses, it is well known—see, for example, Ref. [15]—that nonlinear susceptibilities make a much more sensitive tool to investigate static and dynamic properties of magnetic assemblies than the linear ones.

The goal of this paper is to consistently study the nonlinear SR in a system of identical single domain (also known as *fine* or *nanosize*) anisotropic ferromagnetic particles dispersed in a solid neutral matrix. This is done by a numeri-

*Corresponding author.
Electronic address: ylr@ylr.icmm.perm.su

cally exact solution of the micromagnetic (Brown) equation which grants a complete allowance for both magnetodynamic and thermal noise effects. Besides its direct range of application, the problem in question makes a case that contributes to the understanding of the generic SR behavior of a bistable system subject to a constant force. In this aspect our results should be considered along with the general theoretical treatment of nonlinear SR given in Ref. [16] and particular predictions on the nonlinear behavior of optical bistable systems [17] and a Josephson junction shorted by a superconducting loop [18].

Actually, the body of the paper is divided into five sections. The first two discuss the static susceptibility and the details of the quadratic expansion of the time-dependent Brown kinetic equation, respectively. Thus, the relevant material parameters and all the necessary mathematical schemes are introduced and explained. In Sec. III, the obtained framework is used to derive, calculate, and analyze the set of the dynamic susceptibilities, linear and quadratic, which are the basic quantities to deal with SR. Also, with the concept of the effective relaxation time, we propose a simple expression for the quadratic susceptibility, and give its justifications. In Sec. IV, in terms of the dynamic susceptibility the properties of the linear magnetic SR in a bias field are discussed. In Sec. V, we formulate the definition for a nonlinear SR and present the dependences of the magnetic quadratic SR on the temperature and the bias field strength. By comparison with the numerical results, we show that for the most part of the range of interest, the approximate expression of Sec. III works very well. When used, it yields the signal-to-noise ratio in a compact form, revealing all its essential temperature, bias-field, and frequency dependences.

I. STATIC QUADRATIC SUSCEPTIBILITY

In the presence of a probing field $\mathbf{H}_p$ and a constant bias field $\mathbf{H}$, the orientation-dependent part of the energy function of a single-domain ferromagnetic grain is

$$U=-Kv(\hat{\mathbf{e}}\cdot\hat{\mathbf{n}})^2-\mu[(\hat{\mathbf{e}}\cdot\mathbf{H})+(\hat{\mathbf{e}}\cdot\mathbf{H}_p)], \tag{1}$$

where $\hat{\mathbf{e}}$ and $\hat{\mathbf{n}}$ are the unit vectors of the particle magnetic moment and anisotropy axis, respectively, K is the effective anisotropy constant (essentially positive for the easy-axis case), and $\mu=Iv$ is the magnitude of the magnetic moment of a single-domain particle with I being its magnetization, and v its volume.

We focus on the longitudinal situation and assume that the imposed fields are collinear and directed along the anisotropy axis $\hat{\mathbf{n}}$. Then the set of the angular variables reduces to the polar angle ϑ of $\hat{\mathbf{e}}$ with respect to $\hat{\mathbf{n}}$. Setting $\cos\vartheta=(\hat{\mathbf{e}}\cdot\hat{\mathbf{n}})=x$, at $H_p=$const for the equilibrium distribution function of the particle magnetic moment one gets

$$W(\hat{\mathbf{e}})=W(x)=Z^{-1}\exp[\sigma x^2+(\xi+\xi_p)x], \tag{2}$$

where the values of the internal (anisotropy) and external magnetic energies are scaled with the thermal energy

$$\sigma=Kv/T,\quad \xi=\mu H/T,\quad \xi_p=\mu H_p/T; \tag{3}$$

hereafter we set the Boltzmann constant k_{B} to unity. The partition integral in Eq. (2) is

$$Z(\sigma,\xi,\xi_p)=2\pi\int_{-1}^{1}\exp[\sigma x^2+(\xi+\xi_p)x]dx. \tag{4}$$

To avoid any confusion later on, we remark that under adopted definitions, all the parameters, viz., σ, ξ, and ξ_p are essentially non-negative.

Expanding expression (2) to second order in ξ_p, one gets

$$W(\hat{\mathbf{e}})=W_0\frac{1+\xi_p x+(1/2)\xi_p x^2}{1+\xi_p\langle x\rangle_0+(1/2)\xi_p^2\langle x^2\rangle_0}; \tag{5}$$

here the brackets labeled with 0 denote the averaging over the ''basic state,'' i.e., the distribution

$$W_0(x)=Z_0^{-1}\exp(\sigma x^2+\xi x),$$

$$Z_0(\sigma,\xi)=2\pi\int_{-1}^{1}\exp(\sigma x^2+\xi x)dx. \tag{6}$$

For an assembly of identical noninteracting particles, that is, our model, the longitudinal magnetization assumes the form $M=c\mu\langle x\rangle$, i.e., a single-particle contribution times particle number concentration c. Here the unlabeled angular brackets denote the averaging with the distribution function W from Eq. (2). When the perturbing (probing) field is weak, one may present the magnetization as

$$M-M_0(H)=\chi H_p+\chi^{(2)}H_p^2,\quad M_0(H)=c\mu\langle x\rangle_0, \tag{7}$$

thus introducing, along with the customary susceptibility χ, the quadratic one $\chi^{(2)}$. Note that owing to the magnetization saturation, $\chi^{(2)}$ must be negative.

On the other hand, using expansion (5), one gets the representation

$$\langle x\rangle=\langle x\rangle_0+\xi_p[\langle x^2\rangle_0-\langle x\rangle_0^2]+\tfrac{1}{2}\xi_p^2[\langle x^3\rangle_0-3\langle x^2\rangle_0\langle x\rangle_0+2\langle x\rangle_0^3]. \tag{8}$$

From Eqs. (5)–(8) explicit relations follow:

$$\chi_0=(\phi I^2/K)\sigma A,\quad A(\xi,\sigma)=\langle x^2\rangle_0-\langle x\rangle_0^2, \tag{9}$$

$$\chi_0^{(2)}=(\phi I^3/K^2)\sigma^2 B,$$

$$B(\xi,\sigma)=\tfrac{1}{2}[\langle x^3\rangle_0-3\langle x^2\rangle_0\langle x\rangle_0+2\langle x\rangle_0^3]. \tag{10}$$

Hereafter, instead of the number concentration c, the dimensionless particle volume fraction $\phi=cv$ is used. Note that by definition

$$A=\partial\langle x\rangle_0/\partial\xi,\quad B=\tfrac{1}{2}\partial^2\langle x\rangle_0/\partial^2\xi. \tag{11}$$

In limiting cases, simple expressions for the coefficients A and B are available. For high temperatures $(\sigma,\xi\ll 1)$ one finds

$$A=(\tfrac{1}{3}+\tfrac{4}{45}\sigma)-(\tfrac{1}{15}+\tfrac{544}{11\,025}\sigma)\xi^2,\quad B=-(\tfrac{1}{15}+\tfrac{544}{11\,025}\sigma)\xi. \tag{12}$$

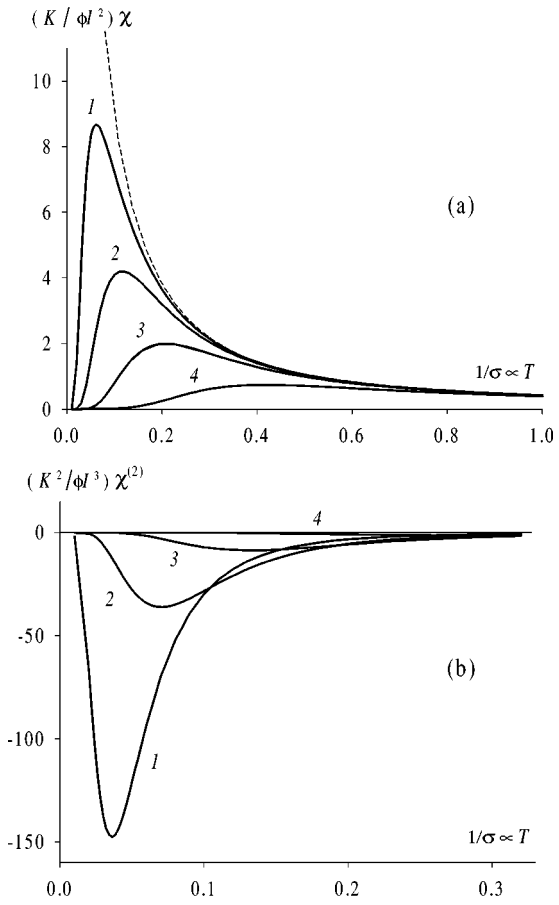

FIG. 1. Static linear (a) and quadratic (b) susceptibilities for the bias field $IH/K = 0.05$ (1), 0.1 (2), 0.2 (3), 0.5 (4). Broken line shows the limiting behavior for $H=0$. Note the factor of 3 difference between the abscissa scales of the (a) and (b) plots.

The low-temperature asymptotics was obtained by Garanin [19]. Namely,

$$A=A_{\text{inter}}+A_{\text{intra}}=\frac{1}{\cosh^2\xi}\,\frac{(2\sigma+\xi)}{(2\sigma-\xi)}+\frac{1}{(2\sigma+\xi)^2}$$

$$\text{for}\quad 2\sigma-\xi\gg 1, \quad (13)$$

and the corresponding B may be found with the aid of definitions (11). The two terms of the right-hand side of Eq. (13) have clear meanings. The first one is caused by redistribution of the particle magnetic moments between the potential minima located at $x=\pm 1$. It may be called the *interwell* contribution. The other is the *intrawell* one, and it accounts for the field-induced orientation inside the deeper well $x=1$, where at $\xi\gg 1$ virtually all the magnetic moments dwell.

According to Eq. (8), the quadratic term is determined by the odd-rank moments of the equilibrium distribution function, and is absent if the latter is even in x. Thus, for the existence of $\chi^{(2)}$ the presence of a bias field in Eq. (1) is mandatory. Otherwise, the next-to-linear response term would be cubic in the probing field amplitude, see Refs. [20], for example.

In Fig. 1 the results of numerical evaluation of static χ and $\chi^{(2)}$ are given for an assembly of uniaxial grains with their axes completely aligned. As the field strength grows, the maxima of the curves move to higher temperatures. A qualitative explanation for this shift may be obtained from Eq. (13). We note that the field strongly affects the temperature behavior of the coefficient A_{inter}. At $H=0$ the interwell contribution is unity and entirely dominates A_{intra}. Then Eq. (9) gives $\chi\propto\sigma\propto 1/T$, i.e., the Curie law shown by a dashed line in Fig. 1(a). For $H\neq 0$, the term A_{inter} in Eq. (13) acquires an exponential factor. Then, on the temperature decrease, an abrupt fall $A_{\text{inter}}\propto\exp(-2\xi)$ takes place. For χ it means that the Curie law gives up, yielding a characteristic maximum. Since $\xi=\mu H/T$, the higher is the field, the greater is the temperature of the maximum. With further cooling, A_{inter} becomes negligible, and the control on the behavior of χ is overtaken by A_{intra}. The occurring crossover—from the exponential to the power law in $1/T$—manifests itself as an inflection point at the leftmost parts of the curves in Fig. 1(a). The same qualitative tendency holds for the quadratic static susceptibilities, see Fig. 1(b).

The discussed static responses are determined for the complete equilibrium. Due to this, they are the easiest to calculate but not at all easy to observe. Indeed, at low temperatures the time needed to achieve the interwell equilibrium becomes exponentially large [21].

II. QUADRATIC EXPANSION OF THE TIME-DEPENDENT DISTRIBUTION FUNCTION

In a nonequilibrium situation, evolution of the distribution function $W(\hat{\mathbf{e}},t)$ is governed by the rotary diffusion (Fokker-Planck-like) equation. In the 1960's Brown [22] specified it for micromagnetic (fine particle) systems. He did this on the basis of the well-known phenomenological Landau-Lifshitz-Gilbert (LLG) equation which describes the magnetodynamics of a single-domain particle in the absence of thermal fluctuations. In a compact vector form the Brown kinetic equation is written [23]

$$2\tau_D\partial W/\partial t=\mathbf{J}W\mathbf{J}(U/T+\ln W), \quad (14)$$

where $\mathbf{J}$ is the operator of infinitesimal rotations with respect to the components of $\hat{\mathbf{e}}$, the energy function U is defined, for example, by Eq. (1), and $\tau_D\propto T^{-1}$ is the reference time of the internal rotary diffusion of the particle magnetic moment. The conventional representation for the diffusion time is

$$\tau_D=\sigma\tau_0, \quad \tau_0=I/2\alpha\gamma K, \quad (15)$$

where γ is the electron gyromagnetic ratio. Here τ_0 is defined through the precession damping parameter α of the underlying LLG equation; see Ref. [24], for example. Qualitatively, τ_0 accounts for the damping effect of the spin-lattice interactions on the orientational motion of $\hat{\mathbf{e}}$. Therefore, τ_0 is the material parameter of a particular system. For us, it yields the decay rate for the intrawell processes, i.e., those occurring near the bottom of the potential wells of $U(x)$. In the presence of the bias field, the intrawell relaxation time modifies to

$$\tau_{\text{intra}}=\tau_0(1+IH/2K)^{-1}. \quad (16)$$

The thermal noise strongly affects the relaxation processes in the superparamagnetic system. At high temperatures, when the presence of the potential wells is insignificant ($\sigma \lesssim 1$), the magnetization relaxation time directly coincides with τ_D, see Eq. (23). In the low-temperature limit ($\sigma \gg 1$), the magnetization reversal takes the form of interwell transitions, and its rate is described by the Néel relation

$$\tau_{\mathrm{N}} = \tau_D \exp(\sigma), \tag{17}$$

with τ_D playing the role of the preexponential factor. The time τ_0 is of a dynamic, not diffusion, origin, and due to that does not depend explicitly upon temperature. It makes it a convenient noise-independent time scale. Then, $\Omega\tau_0$ emerges as a natural criterion with regard to which frequency Ω should be considered to be either high or low. For ferromagnetic particles the reference values of τ_0 are usually taken [24–26] as 10^{-10}–10^{-9} s. Hence, all the frequencies up to the range of at least several MHz may be treated as being low.

Let us assume that the probing field H_1 varies harmonically,

$$H_p = \tfrac{1}{2} H_{p0}(e^{i\Omega t} + e^{-i\Omega t}), \tag{18}$$

and seek the solution of the uniaxial Brown equation (14) in the form of a series

$$W(x,t) = \frac{1}{2\pi} \sum_{l=0}^{\infty} \frac{2l+1}{2} \langle P_l \rangle P_l(x), \tag{19}$$

where $\langle P_l \rangle$, with P_l being the Legendre polynomial, is in fact a conventional notation for the expansion coefficients. As has been mentioned, we restrict ourselves to the low-frequency condition $\Omega\tau_0 \ll 1$. In this limit, the Larmor precession of the particle magnetic moment may be neglected, and Eq. (14) describes a well-overdamped angular oscillator in the bistable potential (1).

Substituting Eq. (19) into Eq. (14), and then integrating over $\hat{\mathbf{e}}$, one arrives at the pentadiagonal set of differential recurrence relations for the mean Legendre polynomials:

$$2\tau_D \frac{d}{dt}\langle P_l \rangle + l(l+1)\langle P_l \rangle - 2\sigma \left[\frac{(l-1)l(l+1)}{(2l-1)(2l+1)} \langle P_{l-2} \rangle + \frac{l(l+1)}{(2l-1)(2l+3)} \langle P_l \rangle - \frac{l(l+1)(l+2)}{(2l+1)(2l+3)} \langle P_{l+2} \rangle \right] - (\xi + \xi_p) \frac{l(l+1)}{2l+1} [\langle P_{l-1} \rangle - \langle P_{l+1} \rangle] = 0. \tag{20}$$

Taking into account that the dimensionless amplitude ξ_{p0} [see scaling (3)] of the probing field is small, the response of the periodically driven system may be found by the perturbation method. To be able to obtain the quadratic susceptibility, we have to perform the pertinent calculation up to the second order in ξ_{p0}. Dealing with the harmonic field (18), we introduce the time-independent complex amplitudes as

$$\langle P_l \rangle - \langle P_l \rangle_0 = \tfrac{1}{2}(b_l^{(1)} e^{i\Omega t} + \text{c.c.}) + \tfrac{1}{4}(b_l^{(2)} e^{2i\Omega t} + \text{c.c.}), \tag{21}$$

where c.c. stands for complex conjugates. On substituting this expansion into Eq. (20), one gets the equation for the complex amplitudes

$$2ik\Omega\tau_D b_l^{(k)} + \sum_{l'} \Lambda_{l,l'} b_{l'}^{(k)} = \xi_{p0} \frac{l(l+1)}{2l+1} [b_{l-1}^{(k-1)} - b_{l+1}^{(k-1)}], \tag{22}$$

valid for the perturbations $b_l^{(k)} \propto \xi_{0p}^k$ from Eq. (21). The operator $\hat{\Lambda}$ in Eq. (22) is the pentadiagonal relaxational matrix whose definition follows from Eq. (20). As usual, the right-hand side of Eq. (22) contains the result of the preceding iteration.

One remark concerning the zeroth order is worthwhile. There one deals with the equilibrium quantities $\langle P_l \rangle$ which can be found from the equation

$$\sum_{l'} \Lambda_{l,l'} \langle P_{l'} \rangle_0 = 0. \tag{23}$$

Its nontrivial solution is provided by the identity $\langle P_0 \rangle_0 = 1$. The corresponding term may be passed to the right-hand side of Eq. (23) thus making this equation nonhomogeneous. In all the higher perturbation orders, $b_0^{(k)} = 0$ identically.

The sets of the pentadiagonal recurrence relations (22) and (23) truncated at some large enough $l = N$, are solved numerically with the aid of the generalized Thomas algorithm, see Ref. [27], for example. Using this algorithm for backward sweeping, that is, from tail to head, yields a procedure which, being in fact equivalent to the continued-fraction method proposed by Risken [28], is more feasible for realization. Both methods provide any desired accuracy just by varying the cutoff index number N. In this sense we call the solutions obtained *numerically exact.*

III. DYNAMIC SUSCEPTIBILITIES

The numerically exact solution of Eqs. (22) and (23) determines the representation for the distribution function (19) accurate up to ξ_{p0}^2. Using it in the reduced magnetization $\langle x \rangle$ definition and with allowance for Eq. (7), one can present the magnetic response as a sum of the frequency-dependent contributions as

$$M = M_0 + \tfrac{1}{2}\chi(\Omega) H_{p0} \exp(i\Omega t) + \tfrac{1}{4}\chi^{(2)}(2\Omega) H_{p0}^2 \exp(2i\Omega t) + \text{c.c.}, \tag{24}$$

thus specifying the linear and quadratic complex susceptibilities

$$\chi = \frac{\phi I^2 \sigma}{K} b_1^{(1)}, \quad \chi^{(2)} = \frac{\phi I^3 \sigma^2}{K^2} b_1^{(2)}. \tag{25}$$

Each of them is a function of the bias field ξ and describes the harmonic of magnetization at the pertinent frequency. Note that in Eq. (24), as in Eq. (21) above, we omit the stationary contribution to $\chi^{(2)}$.

To facilitate understanding, let us recall the main features of the linear longitudinal susceptibility of a superparamagnetic system. The general solution of the linear problem (22) can be formally presented as the spectral expansion

$$\chi=\chi_0\sum_{k=1}^{\infty}\frac{w_k}{1+2i\Omega\tau_D/\lambda_k},\quad \sum_{k=1}^{\infty}w_k=1, \tag{26}$$

where the sets of the eigenvalues $\{\lambda_k\}$ of the relaxational operator $\hat{\Lambda}$ are introduced together with the weights $\{w_k\}$ rendering the contributions of the eigenmodes to the linear susceptibility. In Eq. (26) λ_1 is the lowest eigenvalue, and it is the only one that yields the rate of the interwell relaxation. The corresponding relaxation time reads

$$\tau_{\text{inter}}=2\tau_0/\lambda_1. \tag{27}$$

On the other hand, one can try to approximate the magnetization damping process by a single effective relaxation time as

$$\chi=\chi_0(1+i\Omega\tau_{\text{eff}})^{-1}. \tag{28}$$

In the low-frequency limit the exact and approximate susceptibilities must coincide. Matching the expansions of Eqs. (26) and (28) for $\Omega\tau_D\ll 1$, yields

$$\tau_{\text{eff}}=\sum_{k=1}^{\infty}w_k\tau_k,\quad \tau_k=2\tau_D/\lambda_k. \tag{29}$$

The last relationship is in fact the quantitative definition of τ_{eff}. However, in practice it is more feasible to find τ_{eff} from the solution of the recurrence relation [9,29]

$$\sum_{l'}\Lambda_{l,l'}F_{l'}=2\tau_D(\langle P_lP_1\rangle_0-\langle P_l\rangle_0\langle P_1\rangle_0) \tag{30}$$

as $\tau_{\text{eff}}=F_1/A$.

For high temperatures ($\sigma,\xi\ll 1$) the effective relaxation time of Eq. (29) reduces to

$$\tau_{\text{eff}}=\tau_D. \tag{31}$$

In the low-temperature limit, Garanin [19] found a simplified expression

$$\tau_{\text{eff}}=A^{-1}(A_{\text{inter}}\tau_{\text{inter}}+A_{\text{intra}}\tau_{\text{intra}}), \tag{32}$$

where the parameters A are defined by Eq. (13), and the temperature-independent time τ_{intra} is introduced by Eq. (16). The corresponding asymptotic form of the interwell relaxation time (27) is provided by the formula

$$\lambda_1=\pi^{-1/2}\sigma^{3/2}(1-h^2)\{(1+h)\exp[-\sigma(1+h^2)]+(1-h)\exp[-\sigma(1-h^2)]\}, \tag{33}$$

obtained by Aharoni [21]; here $h=IH/2K$.

In Fig. 2 we present the plot of τ_{eff} obtained from the numerical solution of Eq. (30). The coordinates used for this schematic representation are the dimensionless temperature-independent magnetic field $\xi/\sigma=IH/K$ and dimensionless temperature $1/\sigma$. Note also the logarithmic scale of the vertical axis. The plateau at $\sigma\lesssim 2$ shows that at enhanced temperatures the relaxation time does not depend on the details of the potential. At low temperatures, the effective time is strongly temperature dependent. The form of the surface τ_{eff} in the band $\sigma\gtrsim 5$, i.e., reduced temperatures, is very specific.

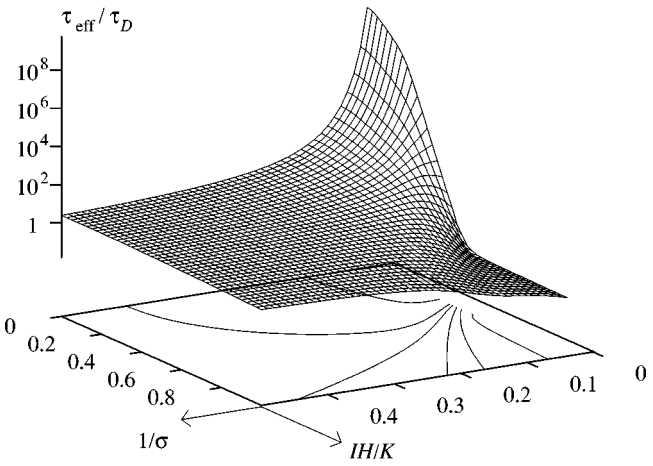

FIG. 2. Integral relaxation time as a function of the dimensionless temperature $1/\sigma$ and bias field strength ξ/σ.

At $\xi=0$ and $1/\sigma\ll 1$ it reduces to τ_{N}, where the Néel relaxation time is defined by Eq. (17). This yields the customary superparamagnetic blocking model with its exponential in $1/T$ behavior. A peculiar feature is the occurrence of a nonmonotonic dependence $\tau_{\text{eff}}(1/\sigma)$ when IH/K exceeds some finite value. This fact was discovered in Refs. [29] and [19], where the evaluation gave $IH/K\approx 0.34$. Remarkably, the similar inflection on the curves $2\tau_D/\lambda_1$ takes place [21] only at IH/K close to 2. This gives a strong direct argument in favor of using τ_{eff}, and not $2\tau_D/\lambda_1$ as the effective relaxation time for the magnetization.

The temperature dependences of χ' and χ'' found by the full numerical procedure [Eqs. (21)–(25)], and with a simple formula (28) but a numerically exact τ_{eff}, are given and compared in Fig. 3 for $\Omega\tau_0=10^{-4}$. We remark that the actual choice of Ω does not matter as long as we deal in the low-frequency range. However, the assumed value seems quite reasonable, since at $\tau_0\sim 10^{-9}$ s it corresponds to the dimensional frequency $\sim 10^4$ Hz that is a convenient measurement range.

As one can see from Fig. 3, the agreement is rather good. Among all, this implies that in the low-frequency domain one can propose a closed equation of the magnetization motion

$$\left(\tau_{\text{eff}}\frac{d}{dt}+1\right)(M-M_0)=\chi_0H_p, \tag{34}$$

where χ_0 is defined by Eq. (9).

From Fig. 3 it follows that the presence of a bias field shifts the maxima of in- and out-phase components of χ in opposite ways: the peaks of the real part move to the higher noise strength region, whereas those of the imaginary parts display the reversed tendency. The behavior of the real part does not differ much from that of the static susceptibility; this is natural since the $\Omega\tau_0$ parameter is small. That is, we observe the dependence of the factor A on ξ described when discussing the static case. The imaginary part of the susceptibility possesses an additional factor $\sim\Omega\tau_{\text{eff}}$ and thus the χ'' behavior is governed by the lowest barrier height, which goes down as the bias field grows.

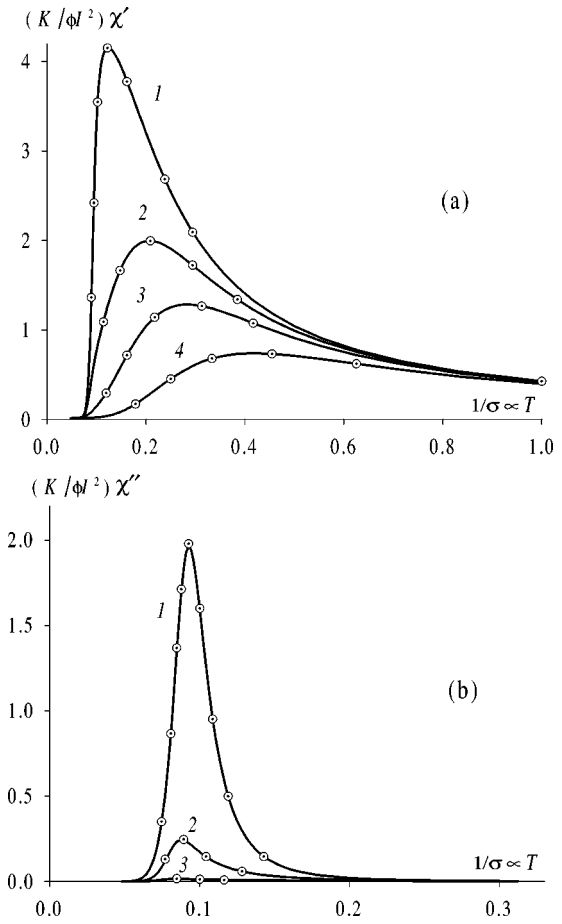

FIG. 3. Real (a) and imaginary (b) parts of the linear dynamic susceptibility at $\Omega\tau_0=10^{-4}$ for the bias field $IH/K=0.1$ (1), 0.2 (2), 0.3 (3), 0.5 (4). For figure (b) the curve with $IH/K=0.5$ does not resolve. Circles show the result of the effective time approximation.

From the general viewpoint, the ability of a relationship such as Eq. (34) to describe the higher harmonics of magnetization is questionable. However, at least for semiquantitative results, one can obtain a useful approximation for $\chi^{(2)}$. For that, let us rewrite Eq. (34) as

$$\left(\tau_{\rm eff}\frac{d}{dt}+1\right)(M-M_0)=H_p\frac{\partial M}{\partial H}, \tag{35}$$

which actually means replacing M_0 by M. Setting in accordance with Eq. (24)

$$M=M_0+\delta M^{(1)}+\delta M^{(2)},$$

$$\delta M^{(1)}=\chi_0(1+i\Omega\tau_{\rm eff})^{-1}H_p, \quad \delta M^{(2)}\sim H_{p0}^2,$$

from Eq. (35) one gets the equation for the second-order correction:

$$\left(\tau_{\rm eff}\frac{d}{dt}+1\right)\delta M^{(2)}=H_p\frac{\partial}{\partial H}\delta M^{(1)},$$

that finally yields

$$\chi^{(2)}=\tfrac{1}{2}\chi_0^{(2)}[(1+i\Omega\tau_{\rm eff})(1+2i\Omega\tau_{\rm eff})]^{-1}, \tag{36}$$

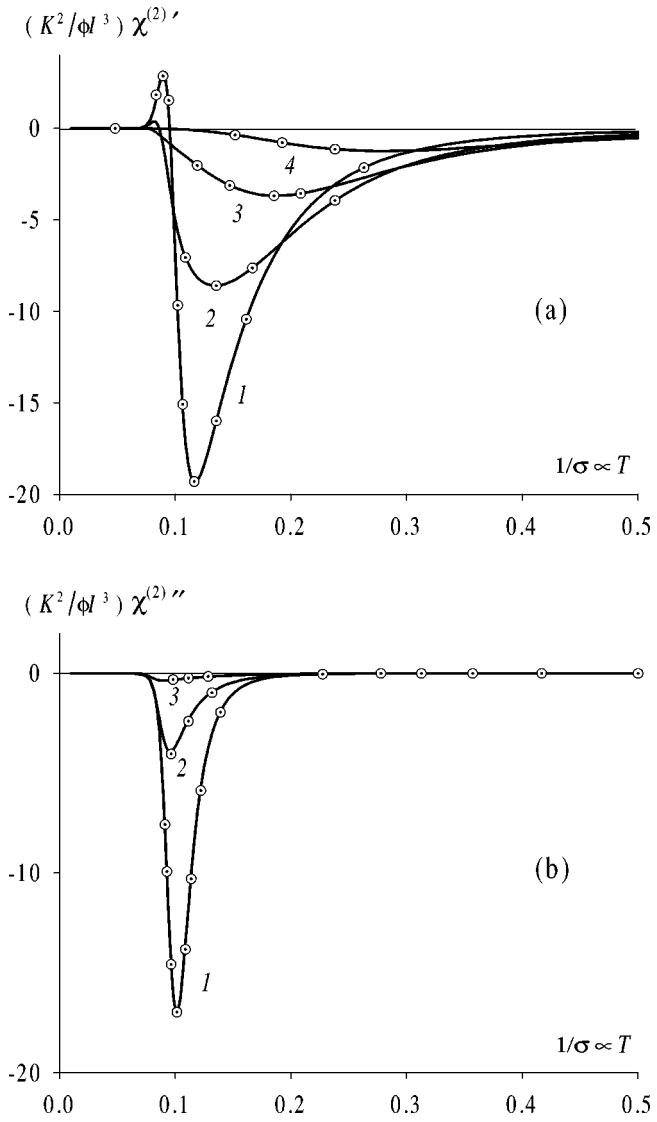

FIG. 4. Real (a) and imaginary (b) parts of the quadratic dynamic susceptibility at $\Omega\tau_0=10^{-4}$ for the bias field $IH/K=0.1$ (1), 0.2 (2), 0.3 (3), 0.5 (4). For figure (b) the curve with $IH/K=0.5$ does not resolve. Circles show the result of the effective time approximation.

where the static value $\chi_0^{(2)}$ is defined in Eq. (10).

The linear susceptibility plots of Fig. 3 may be looked at as a direct illustration of these conclusions. What is less expected is that the effective time approach turns out to be very efficient for the nonlinear response. The justification is given in Fig. 4, where we compare (similarly to Figs. 3) the quadratic susceptibilities evaluated by the numerically exact method and through Eq. (36). All the numerical evidence we have (of which the presented graphical data is just a bit), testifies to the effect that, except maybe for a rather narrow low-temperature range, the effective time approximation rather closely follows the exact solution.

In the plots of quadratic susceptibilities given in Fig. 4 one can notice the same general features as for χ. As for the linear terms, the maxima of $\chi^{(2)\prime}$ and $\chi^{(2)\prime\prime}$ are comparable, and one encounters the same tendency in the peak shifts when the bias field is enhanced. Similarly to the relation between Figs. 1(a) and 1(b), the widths of the imaginary

quadratic plots are smaller than those for the real parts.

Some final remarks on the concept of the effective relaxation time. First, the principle by which $\tau_{\rm eff}$ is defined may be used to introduce similar effective relaxation parameters for perturbations of any higher symmetry as well. But the dipolar case, as δM is, seems to be the most natural. Second, the introduction of $\tau_{\rm eff}$ does not simplify its evaluation. Indeed, according to Eq. (30), to find the effective time, one has to know the solution of the kinetic equation (14). The real gain is in the fact that, as soon as $\tau_{\rm eff}(\sigma,\xi)$ is found, all the dynamic response problems write very simply, making the obtained results compact and easy to analyze. Third, the virtual presence of all the spectral terms in the effective time makes this approach much more adequate than the superparamagnetic blocking model. In the latter, the effective relaxation time of magnetization is identified just with the inverse of the decrement λ_1, which is smallest at $\xi=0$. Such a replacement reduces all the magnetic dynamics to the interwell transition, ignoring all the intrawell ones. Due to that, the blocking model deviates significantly from the exact solution in the low-temperature limit ($\sigma\to\infty$) in the absence of the external field, and also at $\sigma\sim\xi$.

IV. MAGNETIC STOCHASTIC RESONANCE BY THE LINEAR RESPONSE THEORY

Let us first analyze the effect of the bias field on the magnetic SR in the linear response theory approach. The latter was proposed in Refs. [30] and [31] and had considerably clarified the SR concept. The main idea of the linear response treatment is a direct use of the fluctuation-dissipation theorem which expresses the thermal (fluctuational) power spectrum $Q_n(\omega)$ of the magnetic moment of the system, i.e., *magnetic noise*, through the imaginary component of its linear dynamic susceptibility $\mathrm{Im}\chi=-\chi''$ to a weak probing ac field of an arbitrary frequency ω as

$$Q_n(\omega)=(2VT/\omega)\chi''(\omega). \tag{37}$$

Note that all throughout our consideration we use the usual definition of χ as the magnetic susceptibility of a unit volume of the disperse system. Because of that, to keep up with the meaning of the fluctuation-dissipation theorem, in formula (37) the total volume V of the system is introduced. In terms of the total number N of the magnetic particles $V=N/c=Nv/\phi$.

The spectral power density of regular oscillations induced by a driving field of a frequency Ω, i.e., the *signal* in the same terms is written as

$$Q_s(\omega)=\tfrac{1}{2}\pi V^2H_{p0}^2|\chi(\Omega)|^2\delta(\omega-\Omega), \tag{38}$$

where H_{p0} stands for the ac field amplitude. For any real measurement, we get the spectral density in a certain finite frequency bandwidth Δ of the signal detection, that may be accounted for by replacing the delta function by the inverse of the bandwidth.

Upon setting $\omega=\Omega$ in Eqs. (37) and (38), the signal-to-noise ratio (SNR), which is the main issue investigated in the SR theory, may be presented as

$$S=\frac{Q_s}{Q_n}=\frac{\pi N}{4\tau_0\Delta}\left(\frac{IH_{p0}}{K}\right)^2R(\sigma,\xi,\Omega), \tag{39}$$

where the dimensionless function R is introduced to take in all the temperature, frequency, and bias-field strength dependences. Note that in the front factor we use τ_0 instead of τ_D to entirely pass all the temperature dependence to R.

In the effective time approximation (29), from Eqs. (37)–(39) one has

$$R=\sigma^2A\tau_0/\tau_{\rm eff}, \tag{40}$$

revealing, in particular, the absence of the frequency dependence. For a zero bias field ($\xi=0$) and $\sigma>1$ one may set $\tau_{\rm eff}\approx\tau_{\rm N}$ [see Eq. (17)] and recover the most simple relation [4,5] for the linear magnetic SR:

$$R=\sigma^2A\exp(-\sigma). \tag{41}$$

The exact function $R(\sigma,\xi,\Omega)$ in a wide range of its arguments was investigated in Ref. [10] numerically. The method used there, in terms of the present study, is the solution of the set comprising just Eqs. (22), i.e., the linear framework. The comparison has shown that the superparamagnetic blocking model, i.e., the assumption that the system is characterized by a single exponential interwell-passage time $\sim\tau_{\rm N}$, is valid for asymptotic considerations such as Refs. [4] and [5], but is insufficient to find out certain details. In particular, Eq. (41) fails to describe SNR in the zero-temperature limit ($\sigma\to\infty$, $\Omega\tau_{\rm N}\gg1$), and cannot account for either the effect of a bias field or a finite probing frequency value, see Eq. (40).

In Figs. 5 we show (with the appropriate reduction of units) the exact three-dimensional diagrams for Q_s, Q_n, and SNR as derived within the linear response approach from Eqs. (37)–(39), respectively. Note that as the functions of the bias field, both Q terms are maximal at $H=0$ and rapidly decrease with its growth. However, from their sharp peaks located at almost the same point it is difficult to foresee the actual SNR behavior described by the function R shown in Fig. 5(c). It turns out that its maximum is shifted considerably to the right (to higher temperatures) in comparison with those of the susceptibilities, and the rates of change along both axes are much smaller. Note also the massive low-temperature ''shoulder'' of any $R(T)$ curve caused by the intrawell motions, see Ref. [10]. As the bias H grows, this low-temperature plateau widens suppressing the maximum of $R(T)$ which leads to the disappearance of SR itself. This transformation is completed when the bias field exceeds the value $IH/K=2$ above which the potential curve assumes a one-well form.

The results of the effective relaxation time approximation applied to evaluate SNR in the same linear response framework, i.e., by Eq. (40), are shown in Fig. 6. One observes a good agreement with respect to the main cusp of the function $R(T)$. However, in the low-temperature range the existing deviations from the exact solution [they do not resolve in the susceptibility graphs of Fig. 3(a)] become noticeable, see the relative positions of the dots and curve 3 for $1/\sigma<0.1$.

Finishing this section, we would like to formulate explicitly the operational definition of the linear SR measurements

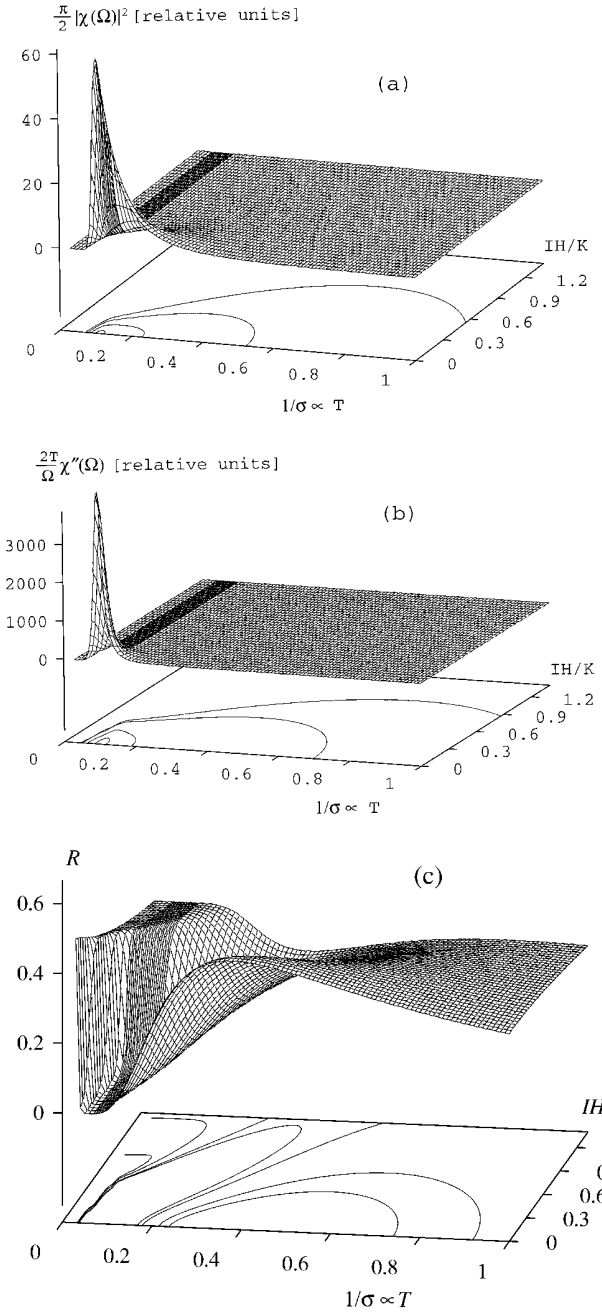

FIG. 5. Signal (a) and noise (b) power densities, and SNR (c) for a superparamagnetic system in the linear response approximation. In the first two figures the vertical scales are chosen to retain only the susceptibility dependences which really matter. Namely, in (a) $(2T/\Omega)\chi''=Q_n/V$, see Eq. (37); in (b) $\frac{1}{2}\pi|\chi|^2=Q_s/V^2H_{p0}^2$, see Eq. (38). In (c) the SNR is characterized by the function R, see Eq. (39). Numerically exact results for the low-frequency case $\Omega\tau_0=10^{-4}$.

that underlies the presented calculation. Namely, we suppose that, first, the equilibrium magnetic power spectrum (no driving ac field) of the system is measured at some frequency Ω after which the driving field would be applied. This quantity is assumed to be Q_n, i.e., the noise. Then the probing ac field is switched on, and the magnetic power density $Q(\Omega)$ is recorded anew. The change in the power density produced by the probing field is considered to be the signal, and we write

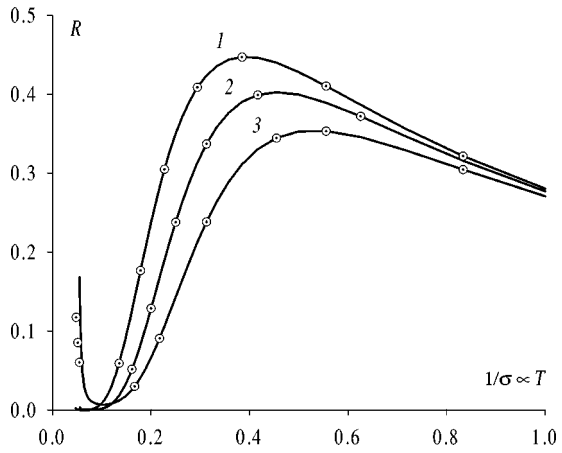

FIG. 6. Comparison of the numerically exact solution (solid lines) and the effective time approximation (circles) with respect to SNR in the linear response approximation; $IH/K=0.1$ (1), 0.3 (2), 0.5 (3). Low-frequency case: $\Omega\tau_0=10^{-4}$.

$$Q(\Omega)=Q_n(\Omega)+Q_s(\Omega). \tag{42}$$

Since Q_n is known from the previous measurement, the signal-to-noise ratio is obtained as

$$S=(Q-Q_n)/Q_n. \tag{43}$$

V. NONLINEAR STOCHASTIC RESONANCE

In Sec. III we showed that the quadratic dynamic susceptibilities of a superparamagnetic system display the temperature maxima which are more sharp than those of the linear ones. If the maximum occurs as well at the temperature dependence of the signal-to-noise ratio, this should be called *the nonlinear* stochastic resonance. However, prior to discussing this phenomenon, one has to define what should be taken as the signal-to-noise ratio in a nonlinear case.

We shall do this with the same kind of the operational definition as in Sec. IV. Namely, we assume that each signal-to-noise value emerges as a result of a three-step action. First, one decides on the frequency Ω at which the test will be performed. Second, at double of this frequency the noise spectral power density in the state with no driving field is evaluated yielding

$$Q_n(2\Omega)=(VT/\Omega)\chi''(2\Omega), \tag{44}$$

[cf. Eq. (37)]. The signal term may be derived directly from the definition

$$Q=\int_{-\infty}^{\infty}\langle\mu(t)\mu(0)\rangle e^{i\omega t}dt. \tag{45}$$

Substituting there the magnetization expansion (24), one obtains

$$\begin{aligned}Q-Q_n&=Q_s(\Omega)+Q_s(2\Omega)\\&=\tfrac{1}{2}\pi V^2[H_{p0}^2|\chi(\Omega)|^2\delta(\omega-\Omega)\\&\quad+H_{p0}^4|\chi^{(2)}(2\Omega)|^2\delta(\omega-2\Omega)],\end{aligned} \tag{46}$$

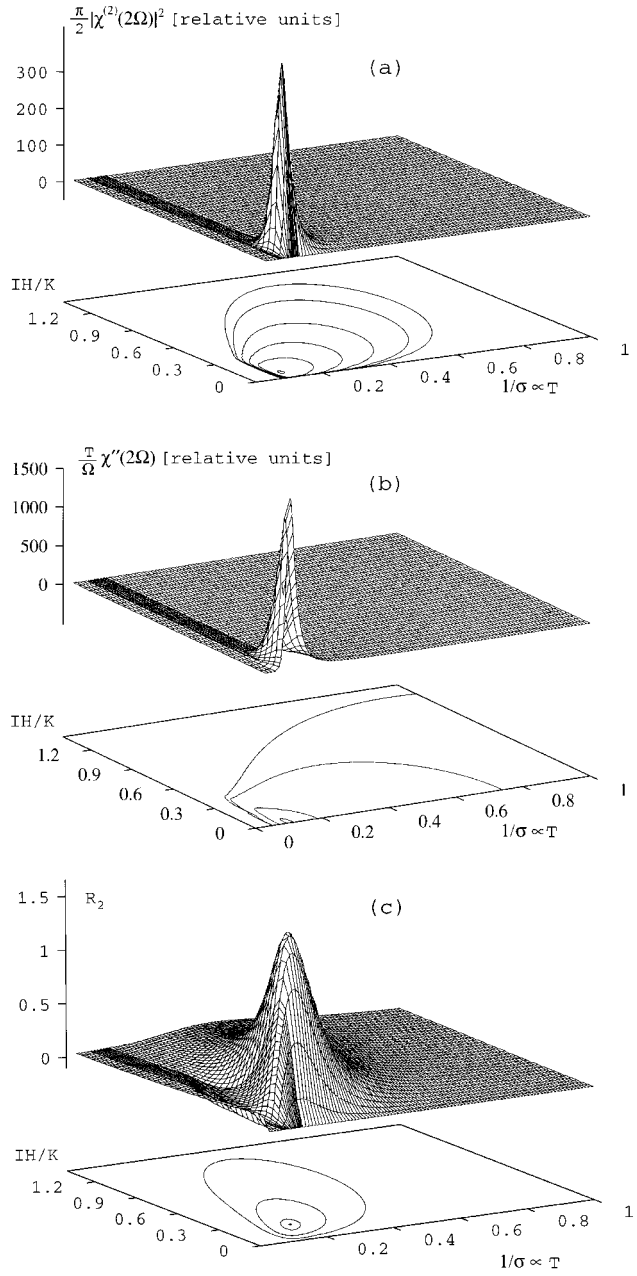

FIG. 7. Signal (a) and noise (b) power densities, and SNR (c) for a superparamagnetic system at the doubled excitation frequency, i.e., quadratic response. In the first two figures the vertical scales are chosen to retain only the susceptibility dependences which really matter. Namely, in (a) $(T/\Omega)\chi''(2\Omega)=Q_n(2\Omega)/V$, see Eq. (44); in (b) $\frac{1}{2}\pi|\chi^{(2)}(2\Omega)|^2=Q_s(2\Omega)/V^2H_{p0}^4$, see Eq. (46). In (c) the SNR is characterized by the function R_2, see Eq. (48). Numerically exact results for the low-frequency case $\Omega\tau_0=10^{-4}$.

where now two terms are field induced. Besides the one of linear origin ($\propto H_{p0}^2$), there appears a fourth-order one stemming from the quadratic response, and rendering the Q component at the double frequency. Using the recipe (43) as a model, we may define the quadratic SR as

$$S_2=[Q(2\Omega)-Q_n(2\Omega)]/Q_n(2\Omega). \tag{47}$$

To extract the dimensional parameters which do not depend explicitly upon temperature, we rearrange the quadratic signal-to-noise ratio to the form

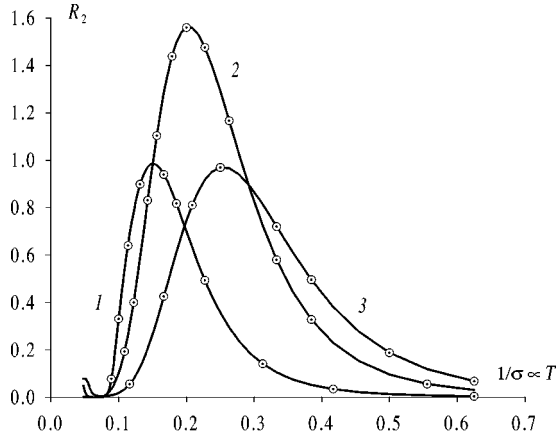

FIG. 8. Comparison of the numerically exact solution (solid lines) and the effective time approximation (circles) with respect to the quadratic SNR; $IH/K=0.1$ (1), 0.3 (2), 0.5 (3). Low-frequency case: $\Omega\tau_0=10^{-4}$.

$$S_2=\frac{\pi N}{16\tau_0\Delta}\left(\frac{IH_{p0}}{K}\right)^4 R_2(\sigma,\xi,\Omega), \tag{48}$$

[cf. Eq. (39)] which is in fact the definition for the function R_2. The latter we obtain through the numerically exact solution of the sets of equations (22) and (23) and its further substitution to Eqs. (25). Note that in the front factor, as in Eq. (39), we use τ_0 instead of τ_D to entirely single out the temperature dependence.

In the effective time approximation described in Sec. III, one can derive the explicit expression

$$S_2=\frac{\pi N}{16\tau_0\Delta}\left(\frac{IH_{p0}}{K}\right)^4 \frac{B^2\sigma^4\tau_0}{A\tau_{\text{eff}}}\,\frac{1}{1+\Omega^2\tau_{\text{eff}}^2}. \tag{49}$$

Remarkable, that even in a simplified approach, such as Eq. (49), the quadratic SR turns out to be essentially frequency dependent.

The inherent feature of the quadratic SR under study is that the bias field is the sole cause of even harmonics in the spectrum. Due to symmetry considerations, they must vanish at $H\to 0$. This means that $S_2(\xi\to 0)=0$. In Eq. (49) this limit is ensured by the proportionality of S_2 to B. According to the second of Eqs. (10), the coefficient B consists only of the odd equilibrium moments of the distribution (6). Since the function W_0 is even in x at $\xi=0$, the odd moments vanish.

On the other hand, at sufficiently high H, the magnetization of the system saturates. This deprives the magnetic moment of any orientational freedom and eventually ''freezes'' it up. Thus, $H\to\infty$ must as well lead to a vanishing response at any harmonic. Under those circumstances, it is clear that the quadratic signal together with SNR, when plotted as functions of the bias field strength, should pass a maximum. The existence of a maximum both at the temperature dependence of the signal-to-noise ratio R_2 (SR at constant H) and the occurrence of the above-described maximum at its bias-field dependence, make it interesting to analyze the quadratic

response above the whole field-temperature coordinate plane. With the developed numerical approach this is easy to carry out, and in Figs. 7 we show the results of such a consideration for $Q_s(2\Omega)$, $Q_n(2\Omega)$, and R_2. The 3D peaks of the spectral density components definitely do not coincide. Due to that, the position and height of the R_2 peak, i.e., the optimized joint action of both dependences, may be found numerically. As Fig. 7(c) shows, it happens to be rather pronounced; see the contour lines at the base plane of the figure. The obtained form of the maximum of R_2 supports the expectation that quadratic SR must be sharper than the linear one, cf. Figs. 5(c) and 7(c).

Figure 8 presents a selection of cross sections of the 3D plot R_2 where we compare the exact solution with the effective time approximation (49). In the low-temperature range the deviations, although not resolved in the graph, are inevitable. But they do not make the main issue of the present study. As to the quadratic SR proper, the agreement again may be pronounced to be excellent.

CONCLUSIONS

A consistent study of the linear and lowest nonlinear (quadratic) susceptibilities of a superparamagnetic system subject to a constant (bias) field is presented. The particles comprising the system are assumed to be uniaxial and identical. The method of study is mainly the numerical solution (exact up to any given accuracy) of the kinetic (Brown) equation. In addition, a simple heuristic expression for the quadratic response is proposed. It uses the recently developed effective relaxation time approximation. The net result is a simple formula of a very good capability that is proved by comparison with the numerical solution.

The application of a constant force (bias field) shifts the position of the ordinary SR peak together with the anticipated reduction of its height and sharpness. For the quadratic SR the situation is more complicated. For it, the joint action of the thermal noise and constant bias results in the formation of a mountainlike surface over the plane of those parameters. In other words, for each given value of the bias field there exists a unique value of the noise strength that maximizes SNR and vice versa. The discovered effect can be useful, for example, for the evaluation of the parameters of bistable systems through susceptibility measurements. In addition, it has to be taken into account when designing any devices where the nonlinear SR is employed.

The studied quadratic SR of a superparamagnetic grain is caused by the interaction of the periodic excitation with the thermal noise. However, there exists an analogy $k_{\mathrm{B}}T \rightarrow \gamma\hbar H_a$, where $H_a = 2K/I$ is the particle anisotropy field, that outlines a passage from thermal to quantum fluctuations. Thus, with certain caution, one may apply the results obtained to the nonlinear SR caused by the tunnel effect at $T=0$.

ACKNOWLEDGMENTS

For Yu.L.R. and V.I.S. this work was supported by RBRF under Grant No. 96-02-16716 of RBRF and by Grant No. 96-0663 from INTAS. A.N.G. acknowledges the support of RBRF under Grant No. 96-02-18956.

[1] K. Weisenfeld and F. Moss, Nature (London) **373**, 33 (1994).
[2] M. I. Dykman *et al.*, Nuovo Cimento D **17**, 661 (1995).
[3] L. Gammaitoni *et al.*, Rev. Mod. Phys. (to be published); Electronic print available at URL http://www.pg.infn.it/sr
[4] A. N. Grigorenko, V. I. Konov, and P. I. Nikitin, Pis'ma Zh. Eksp. Teor. Fiz. **52**, 1182 (1990) [JETP Lett. **52**, 593 (1990)].
[5] E. K. Sadykov, J. Phys.: Condens. Matter **4**, 3295 (1992).
[6] L. B. Kiss *et al.*, J. Stat. Phys. **70**, 451 (1993).
[7] A. N. Grigorenko, P. I. Nikitin, A. N. Slavin, and P. Y. Zhou, J. Appl. Phys. **76**, 6335 (1994).
[8] A. N. Grigorenko, P. I. Nikitin, and G. V. Roschepkin, J. Appl. Phys. **79**, 6113 (1996).
[9] Yu. L. Raikher and V. I. Stepanov, J. Phys.: Condens. Matter **6**, 4137 (1994).
[10] Yu. L. Raikher and V. I. Stepanov, Phys. Rev. B **52**, 3493 (1995).
[11] W. F. Brown, Jr., *Micromagnetics* (Wiley, New York, 1963).
[12] L. Néel, Comptes Rendus **228**, 664 (1949); Ann. Geophys. **5**, 99 (1949).
[13] C. P. Bean and J. D. Livingston, J. Appl. Phys. **30**, 120S (1959).
[14] J.-L. Dormann, D. Fiorani, and E. Tronc, Adv. Chem. Phys. **98**, 283 (1997).
[15] S. L. Ginzburg, *Irreversible Phenomena in Spin Glasses* (Nauka, Moscow, 1989).
[16] Hu Gang, G. Nicolis, and C. Nicolis, Phys. Rev. A **42**, 2030 (1990).
[17] R. Bartussek, P. Hänggi, and P. Jung, Phys. Rev. E **49**, 3930 (1994).
[18] M. E. Inchiosa, A. R. Bulsara, and L. Gammaitoni, Phys. Rev. E **55**, 4049 (1997).
[19] D. A. Garanin, Phys. Rev. E **54**, 3250 (1996).
[20] J. L. García-Palacios and F. J. Lázaro, Phys. Rev. B **55**, 1006 (1997); Yu. L. Raikher and V. I. Stepanov, *ibid.* **55**, 15 005 (1997).
[21] A. Aharoni, Phys. Rev. **177**, 799 (1969).
[22] W. F. Brown, Jr., Phys. Rev. **130**, 1677 (1963).
[23] Yu. L. Raikher and M. I. Shliomis, Zh. Eksp. Teor. Fiz. **74**, 1060 (1974) [Sov. Phys. JETP **40**, 526 (1974)].
[24] M. Sparks, *Ferromagnetic Relaxation* (McGraw-Hill, New York, 1964); *Ferromagnetic Resonance*, edited by S. V. Vonsovskii (Pergamon, Oxford, 1966).
[25] D. P. E. Dickson *et al.*, J. Magn. Magn. Mater. **125**, 345 (1993).
[26] W. Wernsdorfer *et al.*, Phys. Rev. Lett. **78**, 1791 (1997).
[27] C. A. J. Fletcher, *Computational Technique for Fluid Dynamics* (Springer, Berlin, 1988), Vol. 1.
[28] H. Risken, *The Fokker-Planck Equation, Methods of Solutions and Applications* (Springer, Berlin, 1989).
[29] W. T. Coffey, D. S. F. Crothers, Yu. P. Kalmykov, and J. T. Waldron, Phys. Rev. B **51**, 15 947 (1995).
[30] M. I. Dykman, R. Mannella, P. V. E. McClintock, and N. G. Stocks, Phys. Rev. Lett. **65**, 2606 (1990); Pis'ma Zh. Eksp. Teor. Fiz. **52**, 281 (1990) [JETP Lett. **52**, 144 (1990)].
[31] M. I. Dykman, R. Mannella, P. V. E. McClintock, and N. G. Stocks, Phys. Rev. Lett. **68**, 2985 (1992).